



MHD Eyring-Powell fluid flow over a stratified stretching sheet immersed in a porous medium through mixed convection and viscous dissipation

M. Venkata Subba Rao, Kotha Gangadhar & Ali J. Chamkha

To cite this article: M. Venkata Subba Rao, Kotha Gangadhar & Ali J. Chamkha (25 Dec 2023): MHD Eyring-Powell fluid flow over a stratified stretching sheet immersed in a porous medium through mixed convection and viscous dissipation, International Journal of Modelling and Simulation, DOI: [10.1080/02286203.2023.2296678](https://doi.org/10.1080/02286203.2023.2296678)

To link to this article: <https://doi.org/10.1080/02286203.2023.2296678>



Published online: 25 Dec 2023.



Submit your article to this journal [↗](#)



Article views: 54



View related articles [↗](#)



View Crossmark data [↗](#)



Citing articles: 1 View citing articles [↗](#)



MHD Eyring-Powell fluid flow over a stratified stretching sheet immersed in a porous medium through mixed convection and viscous dissipation

M. Venkata Subba Rao^a, Kotha Gangadhar^b and Ali J. Chamkha^c

^aDepartment of Mathematics, School of Applied Science and Humanities, Vignana's Foundation for Science, Technology and Research, Vadlamudi, Andhra Pradesh, India; ^bDepartment of Mathematics, Acharya Nagarjuna University Campus, Ongole, Andhra Pradesh, India; ^cFaculty of Engineering, Kuwait College of Science and Technology, Doha, Kuwait

ABSTRACT

The main aim of the present study is the heat transfer analysis of MHD Eyring-Powell flow over a stratified stretching sheet immersed in a porous material. Mixed convection as well as viscous dissipation effects are considered in order to observe the heat transfer analysis. To strengthen the energy equation viscous dissipation effect is incorporated in this study. Here, temperature distribution is carefully examined to assess rate of heat transmission for the present consideration. Present consideration can have many applications in various engineering fields. Later, the most appropriate similarity transformations are utilized to transform the governing partial differential equations into a nonlinear set of ordinary differential equations. Thereafter, a powerful and convergent procedure namely Runge-Kutta-Fehlberg procedure together with shooting technique is applied to obtain numerical solution for the condensed problem. Graphs are drawn for various values of flow controlling parameters to observe clear insight of the present study through velocity, temperature and concentration profiles. Numerical solutions are tabulated for comparison purpose. The main observations indicate that the temperature and velocity of the fluid decrease over a stretched sheet as the Eyring-Powell fluid material parameter increases. Moreover, mixed convection exhibits a significant impact on the present study, as the parameter value increases. correspondingly, velocity increases, but temperature shows a reverse nature.

ARTICLE HISTORY

Received 13 July 2023
Accepted 14 December 2023

KEYWORDS

MHD; Eyring-powell fluid; viscous dissipation; porous medium; mixed convection and Runge-Kutta-Fehlberg method

1. Introduction

Nowadays researchers have developed a keen interest in studying flow and heat transfer analysis of fluid flows over a stretched surface due to an increase in the use of various scientific and technological advancements in the production of fiber, in textile machinery, in the process of condensation, lubricants, plastic sheets, and food processing and so on. The problem of flow and heat transmission through stretched sheets under various conditions and models has been extensively explored since the seminal work of Crane [1]. Chen [2] performed a reasonable analysis of the laminar mixed convection flow of the boundary layer through a vertically stretched sheet to take into consideration the power law changes in the sheet's temperature and velocity. Later, Chamkha and Mansour [3] analyzed and presented valuable inputs regarding fluid flow over a stretched surface in the presence of a porous medium about the impacts of chemical processes through heat conduction and erratic free convection. Liu et al. [4] distinguished about the heat transfer fluid flow due to an unsteady stretching surface by considering the variable heat flux.

Further, Muhammad et al. [5] gave their valuable and detailed observations regarding Darcy-Forchheimer flow by considering the geometry of exponentially stretching curved surfaces using double diffusion of Cattaneo-Christov impact. In their work, Megahed et al. [6] examined how thermal radiation and heat flux affected laminar flow and heat transfer in an MHD boundary layer over an unevenly stretched sheet.

Magnetohydrodynamic (MHD) flow research captivates scientific interest due to the fascinating impacts that magnetic fields can exert on the boundary layer. To determine the precise similarity solutions, Pavlov considered a homogeneous magnetic field while examining the MHD flow over a stretching surface [7]. Andersson considered and studied an incompressible viscous fluid's MHD flow across a stretching sheet [8]. By studying the MHD flow across an extending permeable surface without and with blowing, respectively [9], and [10] made significant advances in the field. In the long run, especially for high-velocity streams, the model of non-Darcy convection over permeable surfaces makes more sense. Later, esteemed researchers like Tripathi [11] and

Dulal Buddy [12] examined and presented some sensible observations on the MHD boundary layer flow with the help of a non-Darcy model with various geometries. Convection further divides into three subgroups: forced convection, mixed convection, and free convection, often known as natural convection. In this context, researchers [13–17] shared their insightful findings on heat transport analysis using mixed convection with various geometries.

Because of the requirement for non-Newtonian fluids in industry, scientists are currently attempting to understand the consequences of shear stress and fluid flow. A solitary reference equation can't satisfactorily depict the heterogeneous character of non-Newtonian liquids. Stress and strain may not generally correspond directly in non-Newtonian liquids. Since the Eyring-Powell liquid depends on the motor atomic model of fluids instead of an experimental relationship, it is liked above other non-Newtonian fluids. The important role that different fluids play in industries attracts researchers to investigate how they are employed and the challenges that different heat flow phenomena cause. According to Abo-zaid et al. [18], with growing Powell-Eyring fluid parameter values but falling magnetic field values, velocity profiles for both fluid and particle phases rise. The detailed remark by Matthew O. Lawal et al. [19] for mathematical design for Eyring-Powell nanofluid flow gives a wealth of information through the combined impact of non-linear radiation, variable thermal conductivity, and viscosity. Arindam Sarkar et al. [20] looked at temperature-dependent viscosity and thermal conductivity effects on a Powell-Eyring fluid's stretching surface and heat transfer when subjected to nonlinear thermal radiation. Jamshed et al. [21] looked at how a Powell-Eyring nanofluid traveling over a linearly increasing non-uniform medium produced entropy and heat. Bilal and Ashbar [22] distinguished flow and heat transfer in their analysis by considering stratified sheet geometry when Eyring-Powell fluid which is a non-Newtonian fluid flows over stratified sheet by including the mixed convection effect and presented in detail and depth.

Ibrahim et al. [23] employed a model of Cattaneo-Christov heat flux to examine the boundary layer flow of MHD Eyring-Powell nanofluid. The purpose of this research is to examine the close relationship between the concept of mass, energy, momentum conservation, and heat transfer as an input. In their study, Eldabe et al. [24] focused on solving a set of non-linear partial differential equations. These equations are employed to construct a mathematical model, specifically addressing the characteristics of an Eyring-Powell fluid in their investigation. Further, a powerful technique namely FDM is

used to establish the first- and second-order approximations. Malik et al. [25] explored their notable observations about MHD Eyring-Powell fluid, for this they considered the effect of mixed convection with the geometry of stretched plate. They noted their significant observations among them one of the outcomes is a parameter of Eyring-Powell material, the findings show that upgrading greatly lowers in both exchanges they are heat as well as mass.

Furthermore, an in-depth examination of entropy production in the context of Powell-Eyring flow nanofluid immersed in a porous channel was provided by Ogunseye and Sibanda [26], who meticulously designed the mathematical model. To gain insights into the behavior of Eyring-Powell fluid flowing over a stretched sheet using rational Chebyshev functions, Parand and Moayeri [27] conducted a boundary layer investigation through numerical analysis. Salleh et al. [28], utilizing Newtonian theory, conducted heat transfer analyses for a boundary layer flow over a stretched sheet, thereby contributing to the understanding of this phenomenon. In a study by Shuguang Li et al. [29], a comprehensive analysis of the unsteady flow of viscous liquid under the influence of a magnetic field was presented, taking into account the effects of dissipation, ohmic heating, and radiation. Notably, the study delved into the detailed discussion of entropy rate. Furthermore, Zhimeng Liu et al. [30] reported from their investigation that temperature and concentration profiles experience enhancement with increasing Brownian motion. Additionally, as Darcy-Forchheimer and activation energy parameters were elevated, a corresponding reduction was observed in both velocity and concentration profiles. Mamatha et. al [31]. used the Lie group method to analyze the multi-linear regression of a triple diffusive convectively heated boundary layer with the effects of suction and injection.

Further, eminent authors like [32–36] presented their valuable observations on nanofluid flows by considering the various geometries under the influence of various effects. Recently, Xin et. al [37]. reported notable remarks on the problem of minimizing make span for scheduling jobs with equal lengths and arbitrary sizes on uniform parallel batch machines with different capacities. Hadi Jahanshahi et. al [38]. used a unified neural control scheme to get output-constrained trajectory tracking of a space manipulator with the help of unknown parameters and external perturbations. José Luis Díaz Palencia et. al [39]. observed and noted from their study about the wave solutions for Eyring-Powell fluid formulated with a degenerate diffusivity and a Darcy-Forchheimer law. Hayat et. al [40]. investigated the MHD boundary layer flow of Powell-Eyring

nanofluid past a non-linear stretching sheet of variable thickness and presented valid remarks. José Luis Díaz Palencia et. al [41], presented in detail manner about the two-dimensional Eyring-Powell fluid flowing in an MHD porous medium and noted their remarks. Abbas and Ahmed M. Megahed [42] presented valuable observations; one of the observations is that by increasing the thermal stratification parameter cooling process can be controlled considerably.

Shuguang Li et al. [43] presented a mathematical model and explained features in detail about biofiltration treating mixtures of toluene and N-propanol in the biofilm and gas phase. Later, some other important studies regarding various applications, methodologies, and techniques can be seen in Refs [44–46]. Further, Shuhe Sun et al. [47] in their study used the kerosene oil and water base fluid with aluminium oxide and titanium oxide nanoparticles to discuss the thermal phenomenon of the study. Xiao Xin et al. [37] presented detailed observations on Scheduling equal-length jobs with arbitrary sizes on uniform parallel batch machines. Shuguang Li et al. [48] studied the bicriteria problem of scheduling jobs with positional deadlines and agreeable release and processing times on a single machine to minimize total completion time and maximum cost simultaneously. Zhimeng Liu et al. [49] studied very critically and produced a good number of results on Bicriteria multi-machine scheduling with equal processing times subject to release dates.

After carefully studying the studies referenced above, it is felt that the MHD Eyring-Powell fluid model with mixed convection boundary layer flows over a stratified stretched sheet embedded in a porous medium under the influence of viscous dissipation and heat generation/

absorption effects is still lacking in the literature. This model evaluates the behavior of temperature distribution for the proposed fluid flow over a stratified stretched sheet. With the help of suitable similarity transformations governing partial differential equations of the proposed study are transformed into a non-linear system of ordinary differential equations. Thereafter boundary conditions are also transformed into dimensionless form. The Runge-Kutta-Fehlberg procedure together with the shooting technique is applied to obtain a numerical solution for the condensed problem. Tables and graphs are drawn to discuss how various physical characteristics affect each other. For better understating the clear insight of the problem skin friction and the Nusselt number are evaluated numerically. There is a reasonable correlation between the present outcomes and earlier investigations.

This examination aims to find the responses to the following queries: What is the effect of the Eyring-Powell fluid parameter on the velocity of the fluid? Is there any influence on the velocity of Newtonian and non-Newtonian fluid fluids? How does the magnetic field affect the temperature of the fluid? Does the Eckert number influence the temperature of the fluid? How do you solve a nonlinear system of partial differential equations numerically? And does the mixed convection parameter influence the velocity of the fluid?

2. Problem formulation

Let us consider a two-directional, incompressible, steady mixed convection flow of Eyring-Powell fluid when it flows over a stratified stretching sheet as shown in Figure 1. Furthermore, with a constant rate sheet extending perpendicular to the x-axis direction.

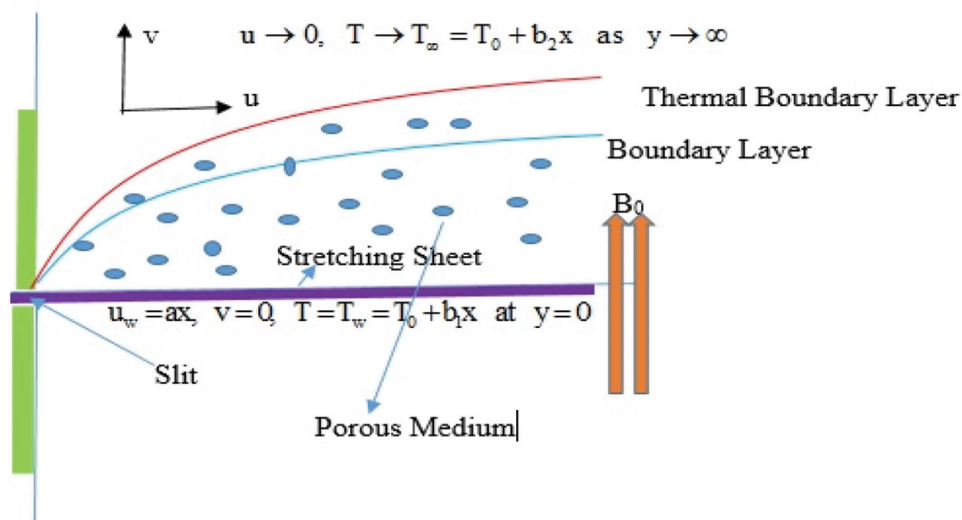


Figure 1. Physical model and coordinate system.

Fluid velocity at the free stream stage is zero. To examine the heat exchange analysis energy equation is strengthened by including the heat generation/absorption effect and viscous dissipation.

For this study, the governing flow equations are as follows and simplified using appropriate boundary layer approximations, as demonstrated in previous works (e.g. Powell and Eyring [50], Kumarans and Srinivas [51], Ramzan et al. [52]).

$$\frac{\partial u}{\partial x} + \frac{\partial v}{\partial y} = 0, \quad (1)$$

$$\begin{aligned} u \frac{\partial u}{\partial x} + v \frac{\partial u}{\partial y} &= \left(v + \frac{1}{\rho\beta C} \right) \frac{\partial^2 u}{\partial y^2} - \frac{1}{2\rho\beta C^3} \left(\frac{\partial u}{\partial y} \right)^2 \frac{\partial^2 u}{\partial y^2} \\ &+ g\beta(T - T_\infty) - \frac{\sigma B_0^2}{\rho} u - \frac{\nu}{k_p} u, \end{aligned} \quad (2)$$

$$u \frac{\partial T}{\partial x} + v \frac{\partial T}{\partial y} = \alpha \frac{\partial^2 T}{\partial y^2} + \frac{Q}{\rho C_p} (T - T_\infty) + \frac{\nu}{C_p} \left(\frac{\partial u}{\partial y} \right)^2. \quad (3)$$

In the above-mentioned equations, $\alpha = \frac{k}{\rho C_p}$, k shows the fluid thermal conductivity, C_p shows at constant pressure specific heat and Q shows the coefficient of heat generation/absorption, T represents the fluid temperature and T_∞ is the ambient temperature, β and C are the Eyring-Powell fluid parameters, μ is the dynamic viscosity, ν is the kinematic viscosity, ρ is the fluid density, σ is the electrical conductivity, B_0 is the magnetic field applied normal to the fluid flow and g is the gravitational acceleration.

For this study, the following are the conditions of boundary:

$$\left. \begin{aligned} u = u_w = ax, \quad v = 0, \quad T = T_w = T_0 + b_1x \quad \text{at} \quad y = 0, \\ u \rightarrow 0, \quad T \rightarrow T_\infty = T_0 + b_2x \quad \text{as} \quad y \rightarrow \infty \end{aligned} \right\} \quad (4)$$

In the above-mentioned equations, both u and v represent the x - and y -axis velocity components, respectively. T_0 , b_1 and b_2 represent the stretching sheet reference temperature related and positive dimensional constants in order. The similarity transformations for the study are as follows, with references available in previous works (e.g. Bilal and Ashbar [22], Abbas and Ahmed M. Megahed [42]).

$$\begin{aligned} u &= axf'(\eta), \quad v = -\sqrt{av}f(\eta), \quad \eta = \sqrt{\frac{a}{\nu}}y, \quad \theta(\eta) \\ &= \frac{T - T_\infty}{T_w - T_0} \end{aligned} \quad (5)$$

In the above equation, ψ is used to represent the stream function which substantially satisfies the C-R Equations, moreover, it can be formulated as $u = \frac{\partial \psi}{\partial y}$, $v = -\frac{\partial \psi}{\partial x}$, $f(\eta)$ shows a non-dimensional stream function for this flow and η shows a variable of similarity for this study, as well

$$T = b_1x\theta(\eta) \quad \text{and} \quad T_\infty = T_0 + b_2x \quad (6)$$

By these assumptions, Equation 2 -Equation 3 are as follows:

$$(1 + \varepsilon)f'''' - \varepsilon\sigma f''^2 f'''' - f'^2 + ff'' + \lambda\theta - (M + G)f' = 0, \quad (7)$$

$$\frac{\theta''}{\text{Pr}} + \theta'f - \theta f' - e_1 f' + \gamma\theta + \text{Ec}f''^2 = 0. \quad (8)$$

Transformed conditions of the boundary are as follows:

$$\left. \begin{aligned} f(0) = 0, \quad f'(0) = 1, \quad \theta(0) = 1 - e_1 \quad \text{at} \quad y = 0 \\ f'(\eta) = 0, \quad \theta(\eta) = 0 \quad \text{as} \quad \eta \rightarrow \infty \end{aligned} \right\} \quad (9)$$

Where,

$$\begin{aligned} \varepsilon &= \frac{1}{\rho\nu\beta C}, \quad \sigma = \frac{aU_w^2}{2C^2\nu}, \quad \lambda = \frac{g\beta b_1}{a^2}, \quad \text{Pr} = \frac{\nu}{\alpha}, \quad M = \frac{\sigma B_0^2}{\rho a} \\ e_1 &= \frac{b_2}{b_1}, \quad \gamma = \frac{Q}{\rho C_p a}, \quad \text{Ec} = \frac{u_w^2}{C_p(T_w - T_0)}, \quad G = \frac{\nu}{k_p a} \end{aligned} \quad (10)$$

The formulas for local skin friction and Nusselt number in this study are presented in the following equations:

$$C_{fx} = \frac{\tau_w}{\rho u_w^2}, \quad Nu_x = \frac{xq_w}{k(T_w - T_\infty)} \quad (11)$$

here, at the surface τ_w shows fluids usual meaning that is shear stress, q_w is shows fluids flux of heat and it is formulated as $q_w = -k\left(\frac{\partial T}{\partial y}\right)_{y=0}$.

With all the assumptions and their substitutions, the simplified formulas for the non-dimensional coefficient of skin friction and the non-dimensional Nusselt number are as follows:

$$\sqrt{\text{Re}_x} C_f = (1 + \varepsilon)f''(0) - \frac{1}{3}\varepsilon\sigma f''^3(0), \quad Nu_x \text{Re}_x^{-\frac{1}{2}} = -\theta'(0) \quad (12)$$

Table 1. Comparison of coefficient of skin friction ($C_f Re^{1/2}$) for various values ε of σ .

$(C_f Re^{1/2})$ ε	σ	Abbas and Ahmed M. Megahed [42]	Hayat et al. [53]	Present Results
0.1	0.1	0.95601695	0.956017	0.956014
0.2	0.1	0.91796980	0.917970	0.917970
0.3	0.1	0.88322379	0.883224	0.883224
0.1	0.1	0.95601695	0.956017	0.956014
0.1	0.5	0.96486289	0.964862	0.9648761
0.1	1.0	0.97531099	0.975312	0.975310

moreover, $Re_x = u_w x / \nu$ represents the formulae for Reynolds number of this study.

3. Solution of the problem

To numerically solve the transformed Equation 7 - Equation 8 with suitable boundary conditions, Equation 9, the Runge-Kutta-Fehlberg (R-K-Fehlberg) technique, along with the shooting method, is implemented. Through the following assumptions, the non-linear system is reduced to a first-order system to implement the proposed method on a simplified system of first-order ordinary differential equations (ODEs). They are as follows:

$$y_1 = f, y_2 = f', y_3 = f'', y_4 = \theta, y_5 = \theta' \quad (13)$$

The resulting differential equations are:

$$y_1' = y_2 \quad (14)$$

$$y_2' = y_3 \quad (15)$$

$$y_3' = \frac{1}{1 + \varepsilon - \varepsilon \sigma^2} (y_2^2 + (M + G)y_2 - y_1 y_3 - \lambda y_4) \quad (16)$$

$$y_4' = y_5 \quad (17)$$

$$y_5' = Pr(y_4 y_2 + e_1 y_2 - y_5 y_1 - \gamma y_4 - Ec y_5^2) \quad (17)$$

Corresponding boundary conditions are:

$$\begin{aligned} y_1(0) = 0; y_2(0) = 0; y_3(0) = a_1; y_4(0) = 1 - e_1; \\ y_5(0) = a_2; y_2(\infty) \rightarrow 0; y_4(\infty) \rightarrow 0 \end{aligned} \quad (19)$$

The above reduced system is solved numerically with R-K-Fehlberg by considering suitable values of a_1 and a_2 . The values of a_1 and a_2 are chosen by shooting method such that $y_2(\infty) \rightarrow 0; y_4(\infty) \rightarrow 0$ are fulfilled. This iterative process continues until the required accuracy is achieved, and further adjustments do not significantly impact the solution. The number of steps and the

size of the starting mesh points are adjusted based on the numerical value of η_∞ . This value is chosen as 6. Furthermore, this study's error tolerance is 10^{-9} . There is a coherent correlation between the results obtained. The Runge-Kutta-Fehlberg method proves advantageous due to its error control mechanism and the ability to adjust the time step to maintain errors within a predetermined range. The numerical outcomes suggest that the proposed method exhibits superior computational speed and provides more accurate results compared to some other existing methods.

3.1 Validation of results and method

For validation purposes of the proposed study and strategy, the outcomes which are found from the proposed technique have been compared with the outcomes available in the literature which are produced by eminent researchers in their past studies for very specific situations. Tables 1–2 indicate such outcomes in chronological order. In detail, skin friction values are measured and documented in Table 1 by adjusting the variables and assuming. These findings are then compared to the literature [42,53] and find a credible relationship between the outcomes. Now coming to Table 2, it produces the details concerning the numerical outcomes of $-\theta'(0)$ and $(C_f Re^{1/2})$ by changing the parametric values. Moreover, a decent correlation between the present study and previous studies.

when $M = \lambda = e_1 = Ec = K_p = \gamma = 0$ with the previous studies like Abbas and Ahmed M. Megahed [42] and Hayat et al. [53]

4. Results and discussion analysis part

This division is going to explain the importance of the consideration of the present problem, in this regard, the R-K-Fehlberg approach is used to numerically solve and to examine the MHD Eyring-Powell flow over a stratified stretched sheet which can be placed in a porous medium with a combined consequence of convection and viscous dissipation. All of the numerical computations are

Table 2. Impact of different parameters on skin friction coefficient and Nusselt number.

ϵ	σ	λ	Pr	e_1	γ	M	K_p	Ec	Skin friction	Nusselt number
0.1	0.1	0.1	0.7	0.3	0.1	0.1	0.1	0.1	1.016002	0.695951
0.3									0.939874	0.722028
0.5									0.878324	0.743727
0.1	0.3								1.020601	0.695376
	0.5								1.025355	0.694791
	0.1	0.3							0.956838	0.713417
		0.5							0.900547	0.727722
		0.1	0.5						0.888080	0.650402
				0.5					0.967628	0.686919
					0.3				0.891650	0.666435
					0.5				0.878817	0.592949
						0.3			0.983654	0.704768
						0.5			1.062097	0.683367
							0.3		0.983654	0.704768
							0.5		1.062097	0.683367
								0.3	0.896020	0.680927
								0.5	0.891578	0.635053

completed for several numerical values of the flow-controlling parameters associated with the current topic to gain a thorough understanding of it. Thereafter, velocity and temperature profile graphs are drawn for numerical estimations of parameters of dimensionless all of which are associated with present consideration through the proposed numerical procedure in order to fully understand the physical problem. The parametric values are taken as $\epsilon = 0.1, \sigma = 0.1, \lambda = 0.1, Pr = 0.7, e_1 = 0.3, \gamma = 0.1, M = 0.1, K_p = 0.1, Ec = 0.1$ otherwise specified. Figures 2–20 display a pictorial depiction of the numerical outcomes.

The graph for the velocity field is presented in Figure 2 for an increasing estimation of the parameter of magnetic field M. The velocity curve decreases with

larger estimates of the parameter M; it can be seen in Figure 2. Because of the existence of the magnetic field effect, a substantial resistive force is developed for the flow of fluid, this force is technically termed Lorentz force, as a result, fluid velocity curve decreases. Figure 3 depicts how the magnetic parameter M affects the distribution of temperature. For higher levels of M, temperature profiles exhibit an increasing pattern of behavior. Higher Lorentz forces (resistive forces) are produced when M is increased, and these forces have the ability to convert some thermal energy into heat energy. Consequently, the temperature profile rises.

Figures 4–5 illustrate how the porosity parameter K_p affects the temperature and velocity patterns. When the porosity parameter increases, consequently, it can be

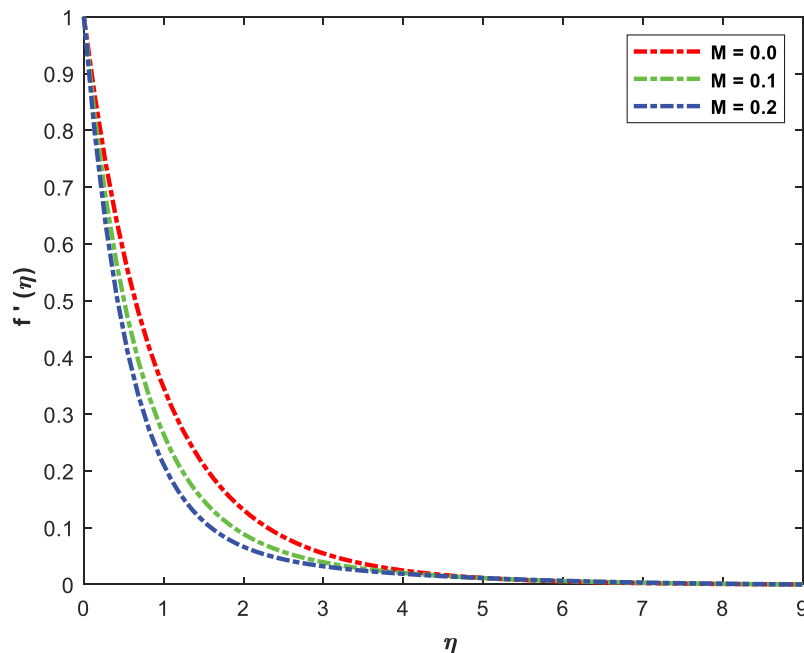


Figure 2. Graph of velocity profile for different values of M.

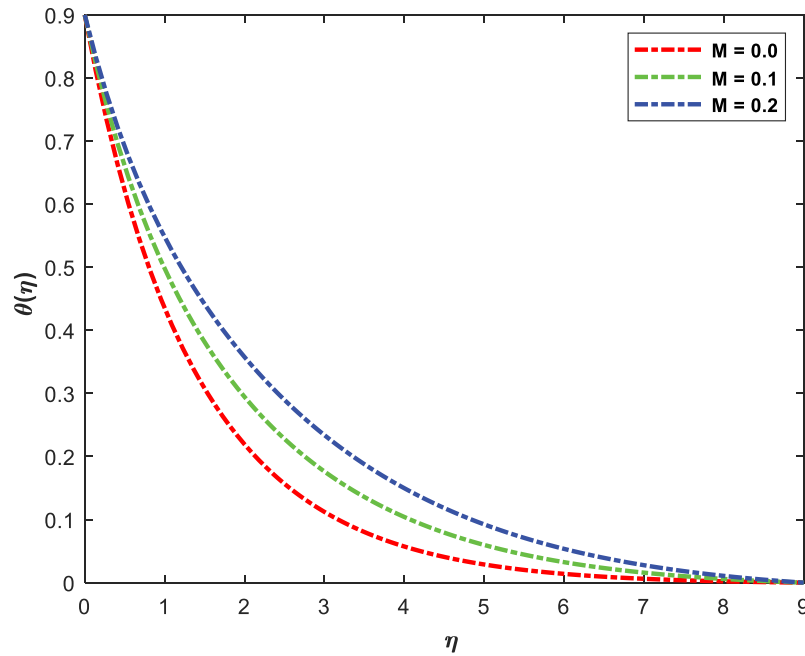


Figure 3. Graph of temperature profile for different values of M .

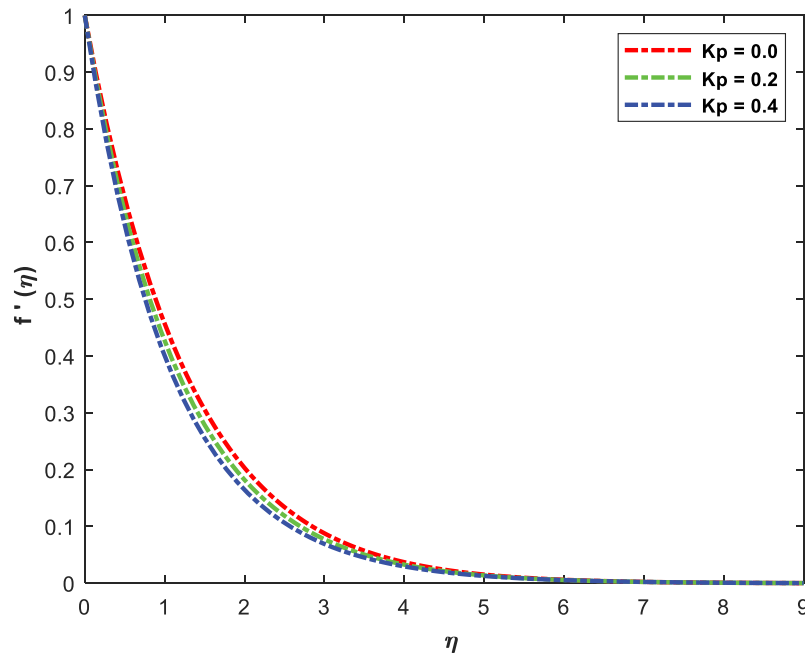


Figure 4. Graph of velocity profile for different values of K_p .

noticed that the velocity profile declines, although the temperature curve exhibits the opposite tendency. The cause of this is that the thermal boundary layer exhibits very modest variations in the heat distribution, which is a weak function of the porosity parameter. The thermal boundary layer therefore gets a little bit thicker as K_p rises. In line with one physical hypothesis, the results will act as a guide for lowering the velocity field,

comparable to fluid flow through a porous medium with a high K_p value.

Figures 6–7 illustrate how temperature and velocity curves change due to the impact of Prandtl number Pr . Actually, from these curves, one can understand that both velocity as well as temperature curves are found to diminish with rising arguments of Pr values. As Pr rises consequently, we can see a decline in the thickness of the

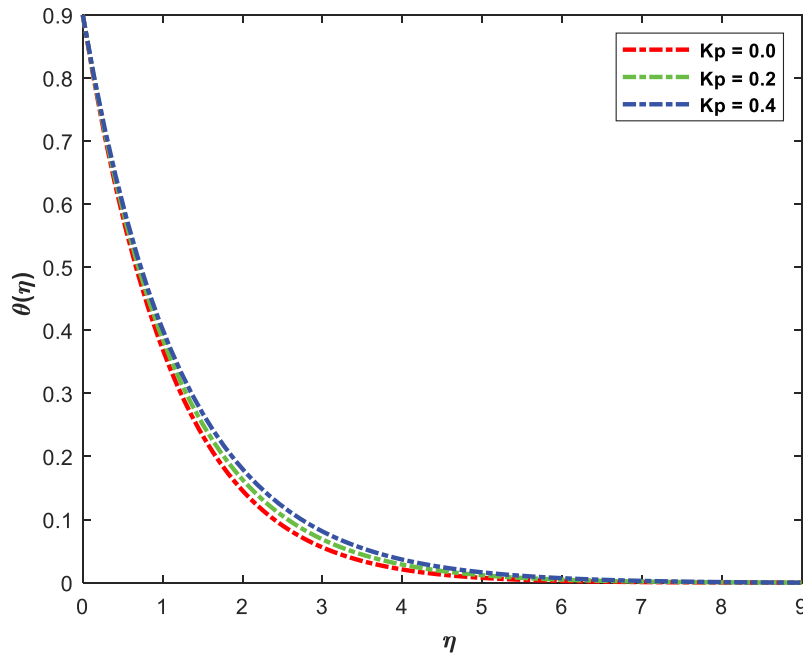


Figure 5. Graph of temperature profile for different values of K_p .

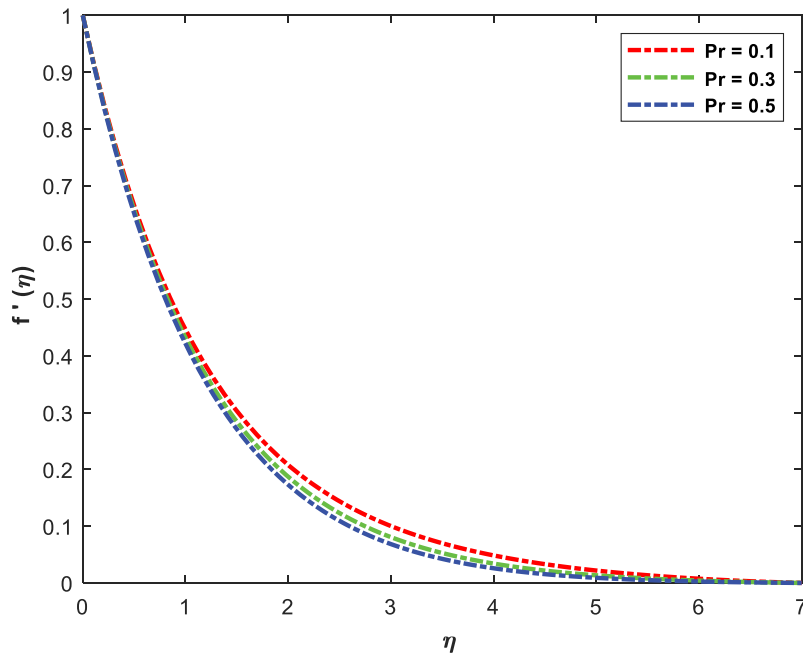


Figure 6. Graph of velocity profile for different values of Pr .

thermal boundary layer. Physically, this is explained by the slower heat transmission of fluids with greater Prandtl values.

In Figures 8–9, the temperature distribution curves for Eckert number Ec values are depicted. The temperature and velocity profiles have increased, as shown in Figures 8–9. As Eckert number Ec increases, associated boundary layers rise as well. This is caused by an increase in heat production as the Eckert number rises,

this is subsequently stored in the fluid, resulting in significant frictional forces between fluid particles. As a result, the temperature distribution becomes more intense.

Figs. 10–11 depict the effect of material parameter σ on combined curves of temperature and velocity. For increasing estimations of the material parameter σ velocity profile is seen to decrease as shown in Figure 10 while the opposite tendency is noted for temperature

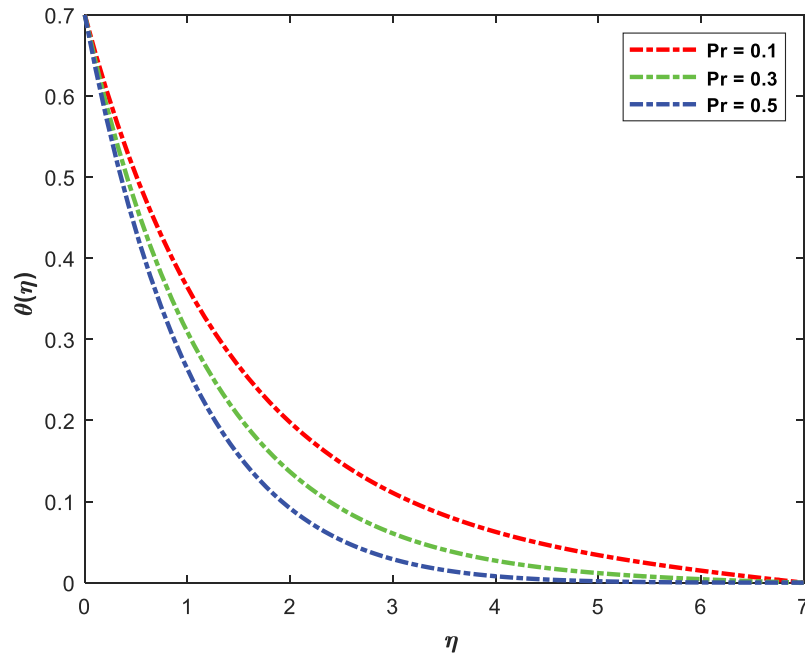


Figure 7. Graph of temperature profile for different values of Pr .

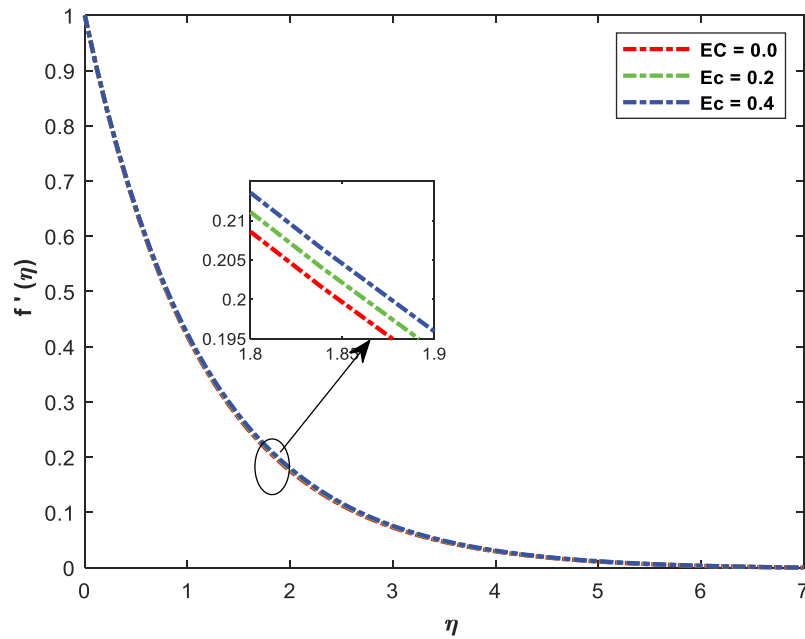


Figure 8. Graph of velocity profile for different values of Ec .

profile for the same increment values of a material parameter as shown in Figure 11.

Figure 12 illustrates the velocity profile for the fluid parameter ε , from this figure it is observed that there is an upsurge in the velocity profile as the fluid parameter ε increases. In contrast, as illustrated in Figure 13, temperature profiles drop off as the value ε increases. The decrease in viscosity of a shear-thinning fluid is associated with an increase in ε . Consequently, fluid molecules move at greater speeds while heat generation is

reduced due to the frictional force. Therefore, the temperature distribution drops.

From Figure 14 it can be identified how the parameter of mixed convection λ changes velocity profile. The graph demonstrates that fluid velocity grows as mixed convection λ increases. This rise was brought by the force of thermal buoyancy. Moreover, noticed that there is an upsurge in the thickness of the momentum boundary layer for variations of buoyancy force. The effect of the mixed convection

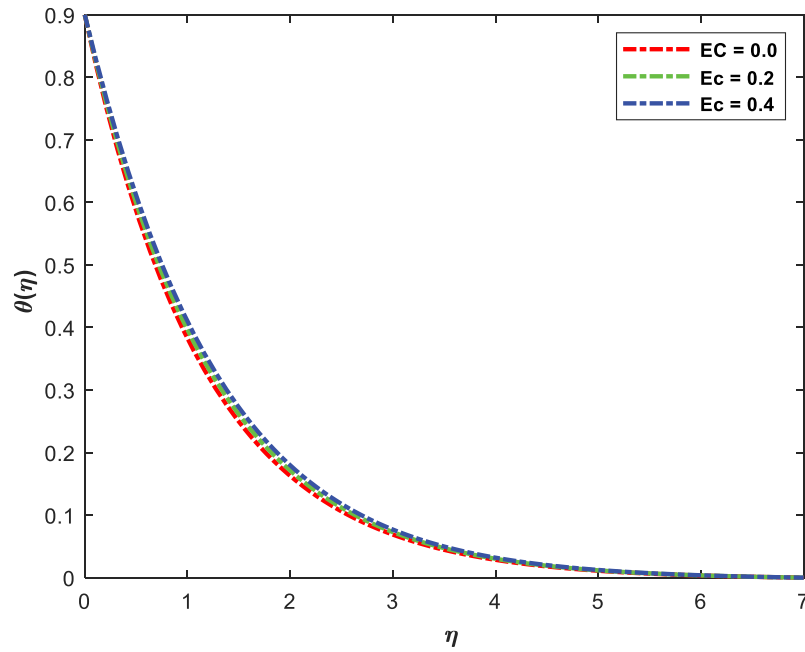


Figure 9. Graph of temperature profile for different values of Ec .

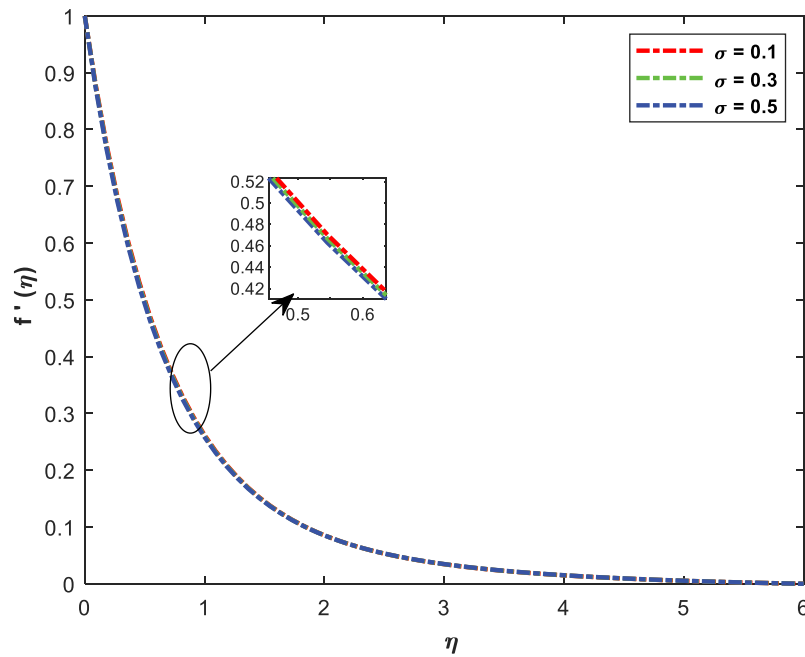


Figure 10. Graph of velocity profile for different values of σ .

parameter on fluid temperature is seen in Figure 15. According to the graph, increasing of λ exhibits a reduction in thermal buoyancy force which lowers the fluid's temperature.

As the heat-generating parameter γ rises, the fluid's velocity across the stretched sheet rises it can be seen in Figure 16. As the heat-generating parameter is raised, the fluid's temperature increases as seen in Figure 17.

Figure 18 illustrates how thermal stratification parameter e_1 behaves on curves of velocity as well as temperature. The graph demonstrates that fluid velocity decreases as temperature stratification upsurges. This phenomenon can be attributed to a reduction in convective potential between the sheet surface and ambient temperature. With an increase in the stratification parameter, the temperature $\theta(\eta)$ of the moving fluid

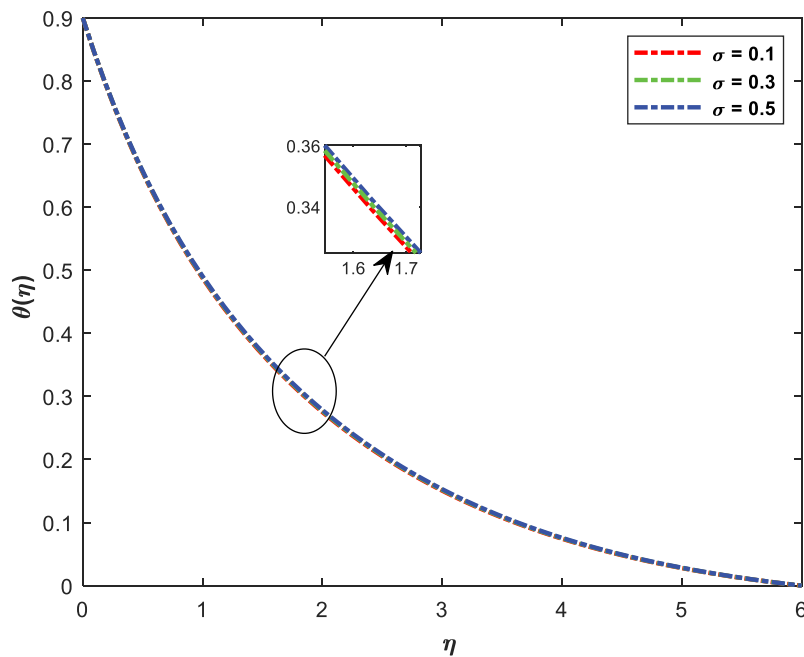


Figure 11. Graph of temperature profile for different values of σ .

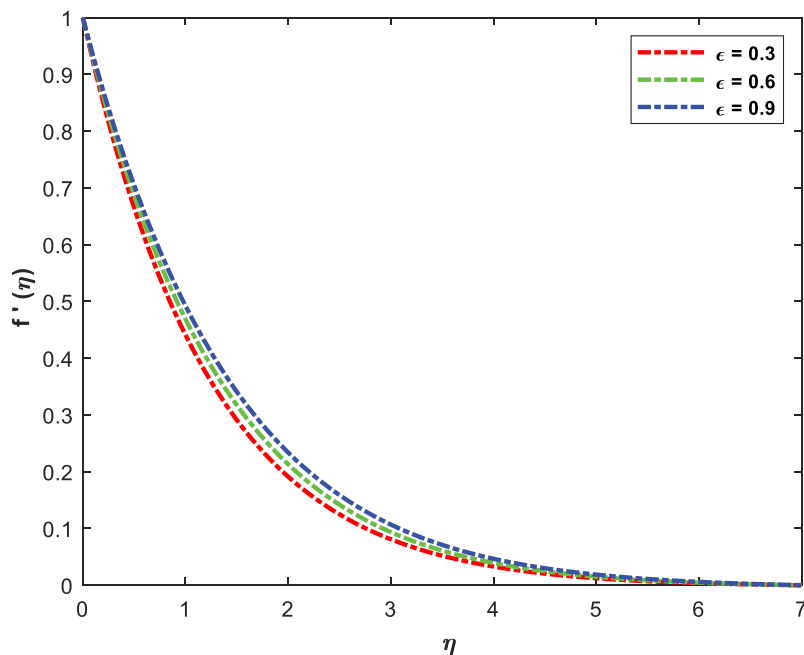


Figure 12. Graph of velocity profile for different values of ϵ .

experiences a decrease. This is because of low temperature difference between the ambient fluid and the fluid at the surface, as depicted in Figure 19.

From Figure 20, it can be noticed that the velocity of Powell-Eyring fluid is greater than the Newtonian model. The reason is that the Powell-Eyring fluid's viscosity decelerates with the shear rate, leading to a rise in both fluid velocity and the thickness of the momentum barrier layer.

5. Conclusions

In this consideration, a numerical approach is employed to examine thoroughly about heat transfer of MHD Eyring-Powell flow over a stratified stretched sheet embedded in a porous medium. Consequently, two effects namely mixed convection and viscous dissipation are included in this study. By using similarity transformations, a nonlinear

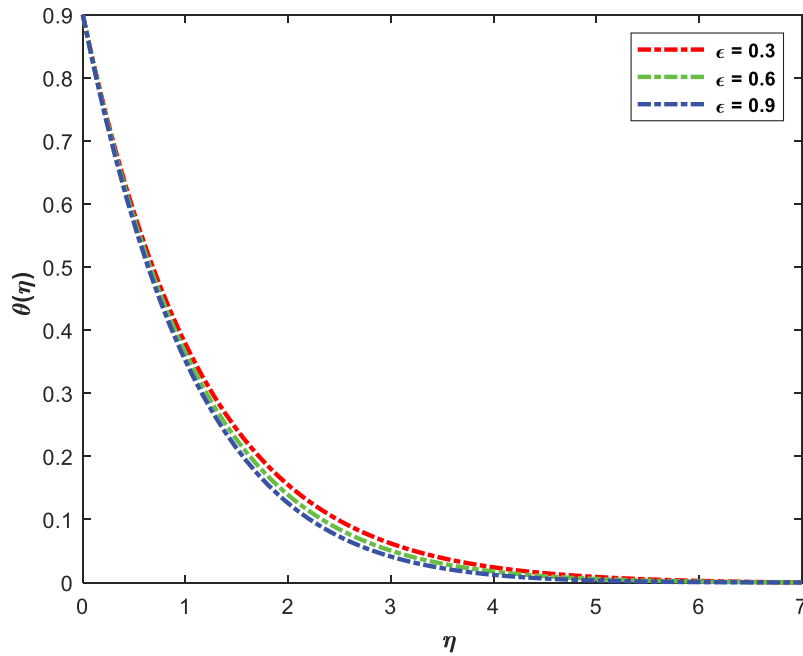


Figure 13. Graph of temperature profile for different values of ϵ .

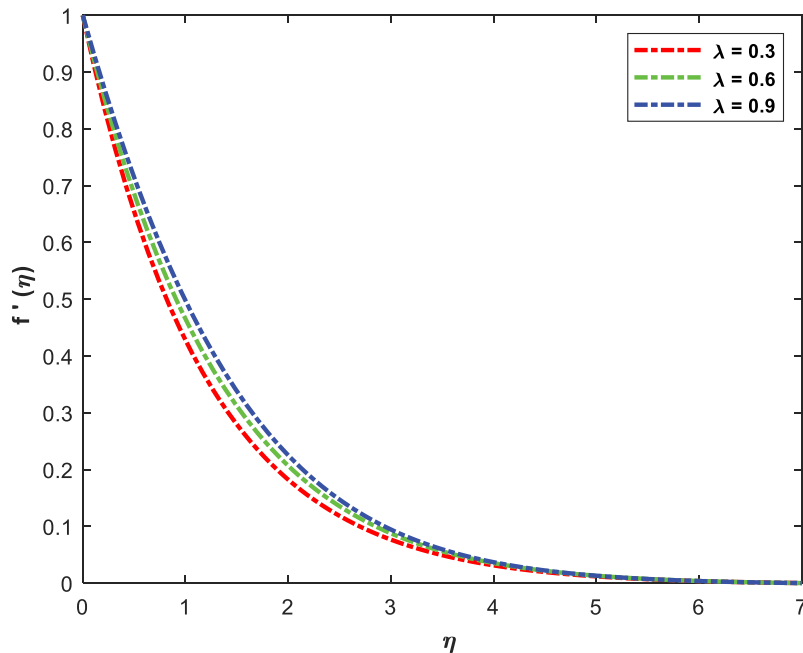


Figure 14. Graph of velocity profile for different values of λ .

system is obtained from governing partial differential equations related to this flow. Using the RKF approach, a numerical solution for the condensed system is obtained. Based on the current investigation numerical results, a reasonable correlation between this analysis and past studies is seen. Some of the findings are

- (1) The Powell-Eyring fluid is compared with the Newtonian model and observed to have more velocity than that of the Newtonian model.
- (2) The heat transfer rate decreases with an increase in the Prandtal number and Eyring-Powell fluid material parameters.
- (3) The temperature and velocity of fluid drops across a stretched sheet are influenced by an increase in the flow-controlling parameter namely Eyring-Powell fluid material.
- (4) As the parameter of Eyring-Powell material is raised, a temperature rise is seen, although the velocity profile falls.

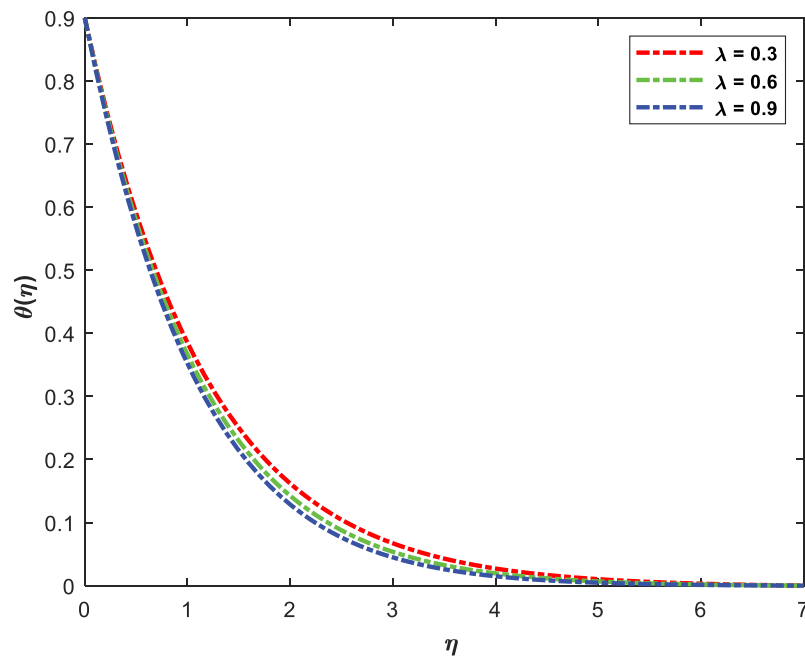


Figure 15. Graph of temperature profile for different values of λ .

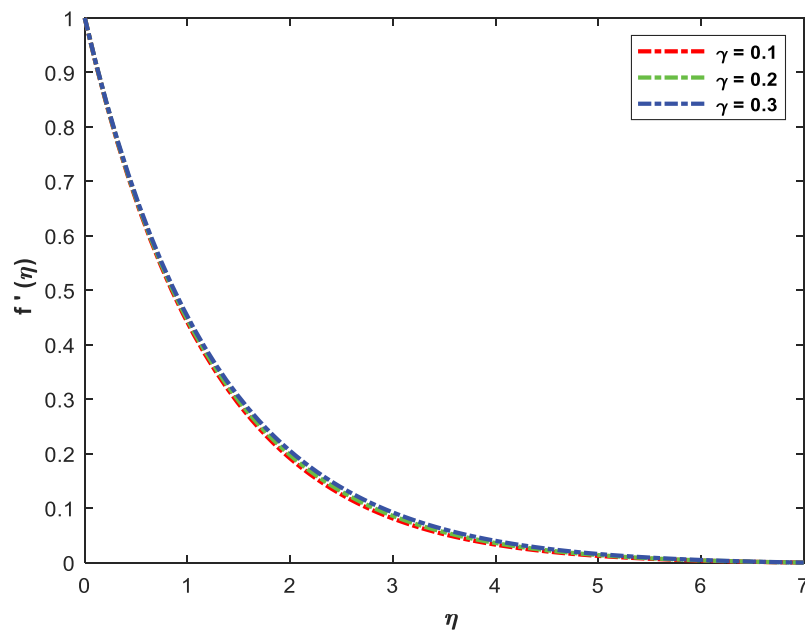


Figure 16. Graph of velocity profile for different values of γ .

- (5) Fluid velocity increases but temperature decreases when the mixed convection value is increased.
- (6) As the Eckert number increases, so does the temperature distribution.
- (7) Fluid velocity decreases while temperature increases as the magnetic parameter is increased.
- (8) As the parameter of porosity is raised, fluid velocity drops while the temperature rises.

- (9) On the basis of the current investigation, a reasonable correlation between this analysis and past studies is seen.

The present study can have applications in the food processing industry, polymer industry, and many engineering fields. With these outcomes, researchers can further modify the problem by including different

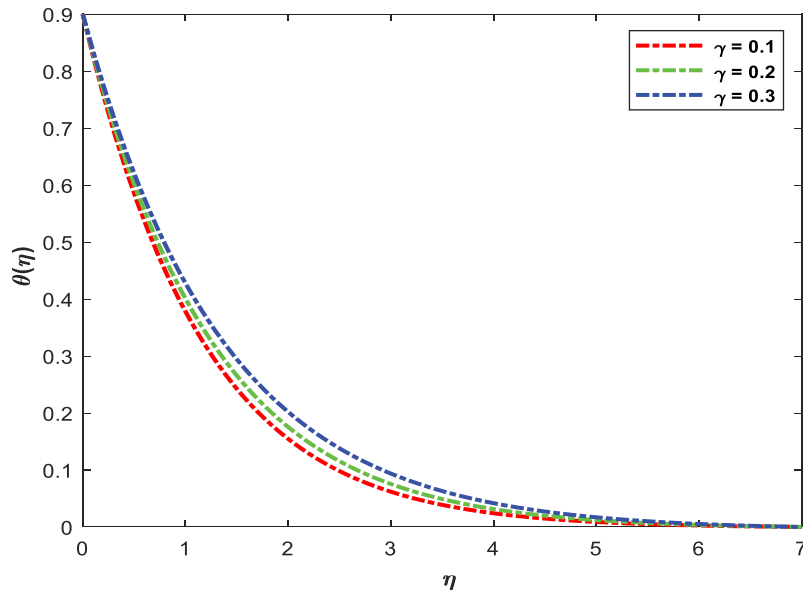


Figure 17. Graph of temperature profile for different values of γ .

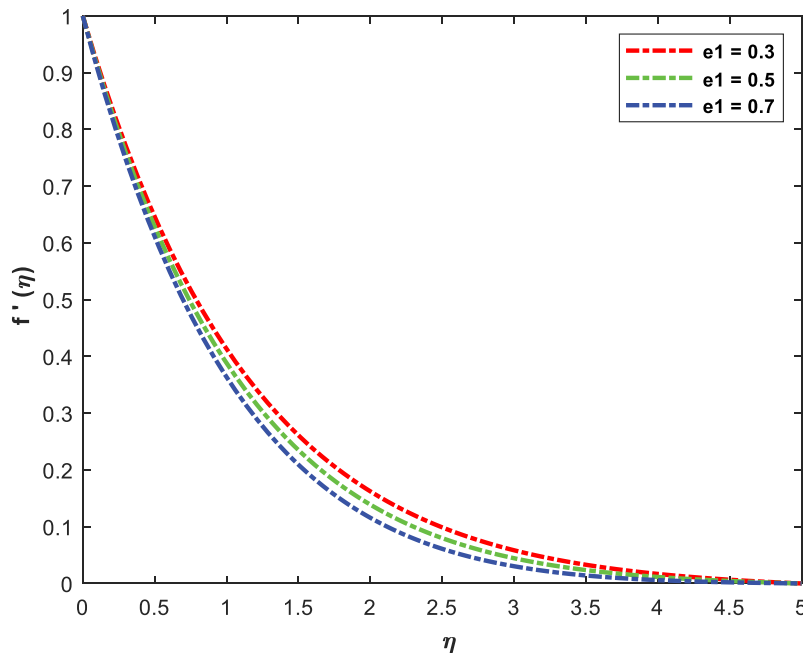


Figure 18. Graph of velocity profile for different values of e_1 .

kinds of thermal flow features like thermal radiation, bioconvection, entropy generation, nonuniform heat source/sink, and so on.

Disclosure statement

No potential conflict of interest was reported by the author(s).

Notes on contributors

Dr. M. Venkata Subba Rao is an Associate Professor in the department of Mathematics at Foundation for Science,

Technology and Research, Vadlamudi, Andhra Pradesh State, India. He earned his Ph.D. in Fluid Dynamics from Foundation for Science, Technology and Research, Vadlamudi, Andhra Pradesh State, India in 2018. His research interest includes MHD, heat and mass transfer and numerical methods. He has 31 publications in archival international journals and conferences.

Dr. Kotha Gangadhar is an Associate Professor in the department of Mathematics at Acharya Nagarjuna University, Andhra Pradesh State, India. He earned his Ph.D. in Fluid Dynamics from Sri Venkateswara University, Andhra Pradesh State, India in 2009. His research interest includes MHD, nanofluid flows over stretching surface and heat and mass

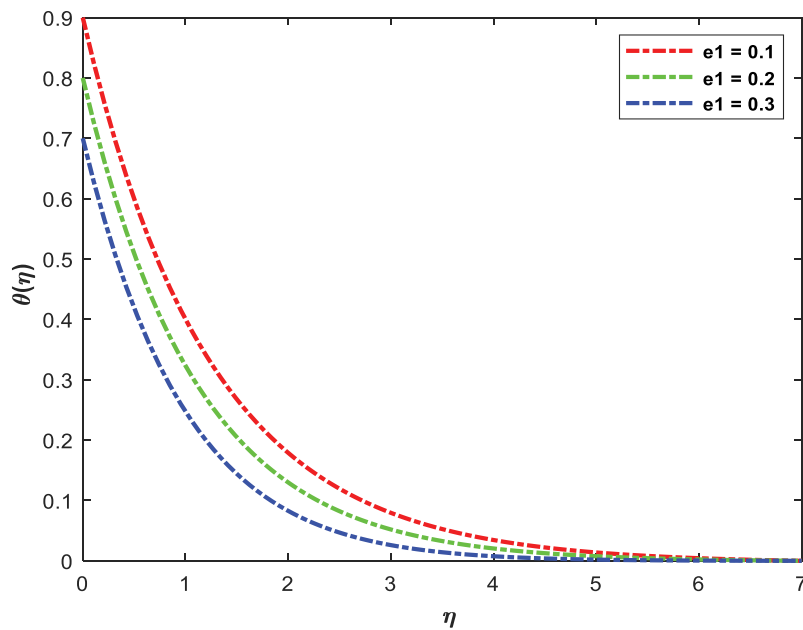


Figure 19. Graph of temperature profile for different values of e_1 .

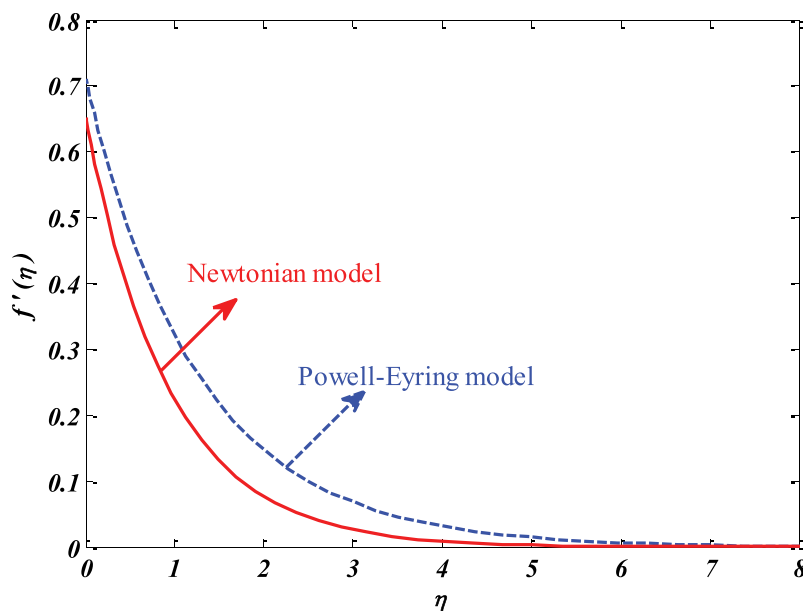


Figure 20. Graph for comparison of Newtonian model vs. Powell - Eyring model.

transfer of non-Newtonian/Newtonian fluids. He has authored and co-authored over 103 publications in archival international journals and conferences. His current h-index is 19 and total citations are 1246.

Prof. Ali J. Chamkha is a Distinguished Professor of Mechanical Engineering and Dean of Engineering at Kuwait College of Science and Technology. He earned his Ph.D. in Mechanical Engineering from Tennessee Technological University, USA, in 1989. His research interests include multiphase fluid-particle dynamics, nano-fluids dynamics, fluid flow in porous media, heat and

mass transfer, magneto hydrodynamics and fluid-particle separation. He has authored and co-authored over 1200 publications in archival international journals and conferences. His current h-index is 130 and total citations are 53,924.

Acknowledgments

The authors are thankful to the honorable editor and anonymous reviewers for their useful suggestions and comments which improved the quality of this paper.

References

- [1] Crane LJ. Flow past a stretching plate. *Z Angew Math Phys.* 1970;21(4):645–647. doi: [10.1007/BF01587695](https://doi.org/10.1007/BF01587695)
- [2] Chen CH. Laminar mixed convection adjacent to vertical, continuously stretching sheets. *Heat Mass Transfer.* 1998;33(5–6):471–476. doi: [10.1007/s002310050217](https://doi.org/10.1007/s002310050217)
- [3] Chamkha AJ, Aly AM, Mansour MA. Similarity solution for unsteady heat and mass transfer from a stretching surface embedded in a porous medium with suction/injection and chemical reaction effects. *Chem Eng Commun.* 2010;197(6):846–858. doi: [10.1080/00986440903359087](https://doi.org/10.1080/00986440903359087)
- [4] Liu IC, Megahed AM, Wang H-H. Hung-Hsun Wang, heat transfer in a liquid film due to an unsteady stretching surface with variable heat flux. *J Appl Mech.* 2013;80(4):041003. doi: [10.1115/1.4007966](https://doi.org/10.1115/1.4007966)
- [5] Muhammad T, Rafique K, Asma M, et al. Darcy–Forchheimer flow over an exponentially stretching curved surface with Cattaneo–Christov double diffusion. *Phys A Stat Mech Appl.* 2020;556:123968. doi: [10.1016/j.physa.2019.123968](https://doi.org/10.1016/j.physa.2019.123968)
- [6] Megahed AM, Gnaneswara MR, Abbas W. Modeling of MHD fluid flow over an unsteady stretching sheet with thermal radiation, variable fluid properties and heat flux. *Math Comput Simul.* 2021;185:583–593. doi: [10.1016/j.matcom.2021.01.011](https://doi.org/10.1016/j.matcom.2021.01.011)
- [7] Pavlov KB. Magnetohydrodynamic flow of an incompressible viscous fluid caused by deformation of a plane surface. *Magn Gidrodin.* 1974;4(1):146–147. doi: [10.22364/mhd](https://doi.org/10.22364/mhd)
- [8] Andersson HI. MHD flow of a viscoelastic fluid past a stretching surface. *Acta Mech.* 1992;95(1):227–230. doi: [10.1007/BF01170814](https://doi.org/10.1007/BF01170814)
- [9] Ioan P, Tsung-Yen N. A note on MHD flow over a stretching permeable surface. *Mech Res Commun.* 1998;25(3):263–269. doi: [10.1016/S0093-6413\(98\)00037-8](https://doi.org/10.1016/S0093-6413(98)00037-8)
- [10] Bhattacharyya K, Layek GC. Chemically reactive solute distribution in MHD boundary layer flow over a permeable stretching sheet with suction or blowing. *Chem Eng Commun.* 2010;197(12):1527–1540. doi: [10.1080/00986445.2010.485012](https://doi.org/10.1080/00986445.2010.485012)
- [11] Tripathy RS, Dash GC, Mishra SR, et al. Numerical analysis of hydromagnetic micropolar fluid along a stretching sheet embedded in porous medium with non-uniform heat source and chemical reaction. *Eng Sci Technol An Int J.* 2016;19(3):1573–1581. doi: [10.1016/j.jestch.2016.05.012](https://doi.org/10.1016/j.jestch.2016.05.012)
- [12] Pal D, Mondal H. Effect of variable viscosity on MHD non-Darcy mixed convective heat transfer over a stretching sheet embedded in a porous medium with non-uniform heat source/sink. *Commun Nonlinear Sci Numer Simul.* 2010;15(6):1553–1564. doi: [10.1016/j.cnsns.2009.07.002](https://doi.org/10.1016/j.cnsns.2009.07.002)
- [13] Chen C-H. Laminar mixed convection adjacent to vertical, continuously stretching sheets. *Heat Mass Transf.* 1998;33(5–6):471–476. doi: [10.1007/s002310050217](https://doi.org/10.1007/s002310050217)
- [14] Ali ME. The effect of variable viscosity on mixed convection heat transfer along a vertical moving surface. *Int J Therm Sci.* 2006;45(1):60–69. doi: [10.1016/j.ijthermalsci.2005.04.006](https://doi.org/10.1016/j.ijthermalsci.2005.04.006)
- [15] Hayat T, Abbas Z, Pop I, et al. Effects of radiation and magnetic field on the mixed convection stagnation-point flow over a vertical stretching sheet in a porous medium. *Int J Heat Mass Transf.* 2010;53(1–3):466–474. doi: [10.1016/j.ijheatmasstransfer.2009.09.010](https://doi.org/10.1016/j.ijheatmasstransfer.2009.09.010)
- [16] Ali M, Al-Yousef F. Laminar mixed convection from a continuously moving vertical surface with suction or injection. *Heat Mass Transf.* 1998;33(4):301–306. doi: [10.1007/s002310050193](https://doi.org/10.1007/s002310050193)
- [17] Khan M, Salahuddin T, Malik M, et al. Change in viscosity of williamson nanofluid flow due to thermal and solutal stratification. *Int J Heat Mass Transf.* 2018;126:941–948. doi: [10.1016/j.ijheatmasstransfer.2018.05.074](https://doi.org/10.1016/j.ijheatmasstransfer.2018.05.074)
- [18] Abo-Zaid OA, Mohamed RA, Hady FM, et al. MHD Powell–Eyring dusty nanofluid flow due to stretching surface with heat flux boundary condition. *J Egypt Math Soc.* 2021;29(1):14. doi: [10.1186/s42787-021-00123-w](https://doi.org/10.1186/s42787-021-00123-w)
- [19] Lawal MO, Kasali KB, Ogunseye HA, et al. On the mathematical model of Eyring–Powell nanofluid flow with non-linear radiation, variable thermal conductivity and viscosity. *Partial Differ Equ Appl Math.* 2022;5(5):100318. doi: [10.1016/j.padiff.2022.100318](https://doi.org/10.1016/j.padiff.2022.100318)
- [20] Sarkar A, Mondal H, Nandkeolyar R. Hiranmoy Mondal and Raj Nandkeolyar, Powell–Eyring fluid flow over a stretching surface with variable properties. *J Nanofluids.* 2023;12(1):47–54. doi: [10.1166/jon.2023.1908](https://doi.org/10.1166/jon.2023.1908)
- [21] Jamshed W, Eid MR, Nisar KS, et al. A numerical framework of magnetically driven Powell–Eyring nanofluid using single phase model. *Sci Rep.* 2021;11(1):16500. doi: [10.1038/s41598-021-96040-0](https://doi.org/10.1038/s41598-021-96040-0)
- [22] Bilal M, Ashbar S. Flow and heat transfer analysis of Eyring–Powell fluid over stratified sheet with mixed convection. *J Egypt Math Soc.* 2020;28(1):40. doi: [10.1186/s42787-020-00103-6](https://doi.org/10.1186/s42787-020-00103-6)
- [23] Ibrahim W, Hindebu B. Magnetohydrodynamic (mhd) boundary layer flow of Eyring–Powell nanofluid past stretching cylinder with cattaneo-christov heat flux model. *Nonlinear Eng.* 2019;8(1):303–317. doi: [10.1515/nleng-2017-0167](https://doi.org/10.1515/nleng-2017-0167)
- [24] Eldabe N, Hassan A, Mohamed MAA. Effect of couple stresses on the MHD of a non-Newtonian unsteady flow between two parallel porous plates. *Z Naturforsch A.* 2003;58(4):204–210. doi: [10.1515/zna-2003-0405](https://doi.org/10.1515/zna-2003-0405)
- [25] Malik M, Khan I, Hussain A, et al. Mixed convection flow of MHD Eyring–Powell nanofluid over a stretching sheet: a numerical study. *AIP Adv.* 2015;5(11):117118. doi: [10.1063/1.4935639](https://doi.org/10.1063/1.4935639)
- [26] Ogunseye HA, Sibanda P. A mathematical model for entropy generation in a Powell–Eyring nanofluid flow in a porous channel. *Heliyon.* 2019;5(5):e01662. doi: [10.1016/j.heliyon.2019.e01662](https://doi.org/10.1016/j.heliyon.2019.e01662)
- [27] Parand, Moayeri M, Parand LD, et al. A numerical investigation of the boundary layer flow of an Eyring–Powell fluid over a stretching sheet via rational chebyshev functions. *Eur Phys J Plus.* 2017;132(7):325. doi: [10.1140/epjp/i2017-11600-0](https://doi.org/10.1140/epjp/i2017-11600-0)
- [28] Salleh MZ, N R, I P. Boundary layer flow and heat transfer over a stretching sheet with Newtonian

- heating. *J Taiwan Inst Chem Eng.* 2010;41(6):651–655. doi: [10.1016/j.jtice.2010.01.013](https://doi.org/10.1016/j.jtice.2010.01.013)
- [29] Shuguang Li MIK, Alzahrani F, Eldin SM. Heat and mass transport analysis in radiative time dependent flow in the presence of Ohmic heating and chemical reaction, viscous dissipation: an entropy modeling. *Case Stud Thermal Eng.* 2023;42:102722. doi: [10.1016/j.csite.2023.102722](https://doi.org/10.1016/j.csite.2023.102722)
- [30] Liu Z, Shuguang L, Sadaf T, et al. Numerical bio-convective assessment for rate type nanofluid influenced by Nield thermal constraints and distinct slip features. *Case Stud Thermal Eng.* 2023;44:102821. doi: [10.1016/j.csite.2023.102821](https://doi.org/10.1016/j.csite.2023.102821)
- [31] Mamatha SU, Renuka Devi RLV, Ameer Ahammad N, et al. Multi-linear regression of triple diffusive convectively heated boundary layer flow with suction and injection: lie group transformations. *Int J Modern Phys B.* 2023;37(1):2350007. doi: [10.1142/S0217979223500078](https://doi.org/10.1142/S0217979223500078)
- [32] V KH, Thejas R, S NC, et al. A review on electrical and gas-sensing properties of reduced graphene oxide-metal oxide nanocomposites. *Biomass Conv Bioref.* 2022. doi:[10.1007/s13399-022-03258-7](https://doi.org/10.1007/s13399-022-03258-7).
- [33] Chu Y-M, Shaik Jakeer SRRR, Lakshmi Rupa M, et al. Double diffusion effect on the bio-convective magnetized flow of tangent hyperbolic liquid by a stretched nano-material with Arrhenius catalysts. *Case Stud Thermal Eng.* 2023;44:102838. doi: [10.1016/j.csite.2023.102838](https://doi.org/10.1016/j.csite.2023.102838)
- [34] Li, Shuguang, Ali, et al. Bioconvection effect in the Carreau nanofluid with Cattaneo–Christov heat flux using stagnation point flow in the entropy generation: micromachines level study. *Open Physics.* 2023;21(1):20220–20228. doi: [10.1515/phys-2022-0228](https://doi.org/10.1515/phys-2022-0228)
- [35] Li S, Raghunath K, Alfaleh A, et al. Effects of activation energy and chemical reaction on unsteady MHD dissipative Darcy–Forchheimer squeezed flow of Casson fluid over horizontal channel. *Sci Rep.* 2023;13(1):2666. doi: [10.1038/s41598-023-29702-w](https://doi.org/10.1038/s41598-023-29702-w)
- [36] Li S, Puneeth V, Saeed AM, et al. Analysis of the Thomson and troian velocity slip for the flow of ternary nanofluid past a stretching sheet. *Sci Rep.* 2023;13(1):2340. doi: [10.1038/s41598-023-29485-0](https://doi.org/10.1038/s41598-023-29485-0)
- [37] Xin X, Khan MI, Shuguang L. Scheduling equal-length jobs with arbitrary sizes on uniform parallel batch machines. *Open Math.* 2023;21(1):20220562. doi: [10.1515/math-2022-0562](https://doi.org/10.1515/math-2022-0562)
- [38] Jahanshahi H, Yao Q, Ijaz Khan M, et al. Unified neural output-constrained control for space manipulator using tan-type barrier Lyapunov function. *AdvSpace Res.* 2023;71(9):3712–3722. doi: [10.1016/j.asr.2022.11.015](https://doi.org/10.1016/j.asr.2022.11.015)
- [39] Luis Díaz Palencia J, Ur Rahman S, Naranjo Redondo A. Analysis of travelling wave solutions for Eyring-Powell fluid formulated with a degenerate diffusivity and a Darcy-Forchheimer law. *AIMS Math.* 2022;7(8):15212–15233. doi: [10.3934/math.2022834](https://doi.org/10.3934/math.2022834)
- [40] Hayat T, Ikram Ullah AA, Farooq M. MHD flow of Powell-Eyring nanofluid over a non-linear stretching sheet with variable thickness. *Results Phys.* 2017;7:189–196. doi: [10.1016/j.rinp.2016.12.008](https://doi.org/10.1016/j.rinp.2016.12.008)
- [41] Luis Díaz Palencia J, Ur Rahman S, Hanif S. Regularity criteria for a two-dimensional Eyring-Powell fluid flowing in a MHD porous medium. *Elec Res Archive.* 2022;30(11):3949–3976. doi: [10.3934/era.2022201](https://doi.org/10.3934/era.2022201)
- [42] Abbas W, Megahed AM. Powell-Eyring fluid flow over a stratified sheet through porous medium with thermal radiation and viscous dissipation. *AIMS Math.* 2021;6(12):13464–13479. doi: [10.3934/math.2021780](https://doi.org/10.3934/math.2021780)
- [43] Shuguang Li SMC, Sudha PN, Sagar Ningonda Sankeshwari SV, et al. Mathematical modelling of the biofiltration treating mixtures of toluene and N-propanol in the biofilm and gas phase. *Int J Hydrogen Energy.* 2023;48(76):29759–29770. doi: [10.1016/j.ijhydene.2023.03.421](https://doi.org/10.1016/j.ijhydene.2023.03.421)
- [44] Shuguang Li MIK, Rafiq M, Abdelmohsen SAM, et al. Optimized framework for Darcy-Forchheimer flow with chemical reaction in the presence of Soret and Dufour effects: a shooting technique. *Chem Phys Lett.* 2023;825:140578. doi: [10.1016/j.cplett.2023.140578](https://doi.org/10.1016/j.cplett.2023.140578)
- [45] Shuguang Li MIK, Bandar Alruqi A, Ullah Khan S, et al. Entropy optimized flow of Sutterby nanomaterial subject to porous medium: Buongiorno nanofluid model. *Heliyon.* 2023;9(7):e17784. doi: [10.1016/j.heliyon.2023.e17784](https://doi.org/10.1016/j.heliyon.2023.e17784)
- [46] Shuguang L, Waqas MQ, AlQahtani S, et al. Electromagnetic Visco-plastic nanofluid flow considering Buongiorno two-component model in frames of Darcy-Forchheimer porosity. *Trans And Joule Heating, J Magnetics.* 2023. doi: [10.4283/jmag.2023.28.2.187](https://doi.org/10.4283/jmag.2023.28.2.187)
- [47] Shuhe Sun MIK, Al-Khaled K, Raza A, et al. Prabhakar fractional approach for enhancement of heat transfer due to hybrid nanomaterial with sinusoidal heat conditions. *Case Stud Thermal Eng.* 2023;49:103240. doi: [10.1016/j.csite.2023.103240](https://doi.org/10.1016/j.csite.2023.103240)
- [48] Shuguang L, Sun Y, Ijaz Khan M. Single machine pareto scheduling with positional deadlines and agreeable release and processing times. *Elec Res Archive.* 2023;31(5):3050–3063. doi: [10.3934/era.2023154](https://doi.org/10.3934/era.2023154)
- [49] Liu Z, Shuguang L, Ijaz Khan M, et al. Bicriteria multi-machine scheduling with equal processing times subject to release dates. *Netw Heterog Media.* 2023;18(3):1378–1392. doi: [10.3934/nhm.2023060](https://doi.org/10.3934/nhm.2023060)
- [50] Powell R, Eyring H. Mechanisms for the relaxation theory of viscosity. *Nature.* 1944;154(3909):427–428. doi: [10.1038/154427a0](https://doi.org/10.1038/154427a0)
- [51] Kumarans B, Srinivas S. Unsteady hydro magnetic flow of Eyring-Powell nanofluid over an inclined permeable stretching sheet with joule heating and thermal radiation. *J Appl Comput Mech.* 2020;6:259–270. doi: [10.22055/JACM.2019.29520.1608](https://doi.org/10.22055/JACM.2019.29520.1608)
- [52] Ramzan M, Bilal M, Kanwal S, et al. Effects of variable thermal conductivity and non-linear thermal radiation past an eyring powell nanofluid flow with chemical reaction. *Commun Theor Phys.* 2017;67(6):723–731. doi: [10.1088/0253-6102/67/6/723](https://doi.org/10.1088/0253-6102/67/6/723)
- [53] Hayat T, Ali S, Farooq MA, et al. On comparison of series and numerical solutions for flow of Eyring-Powell fluid with newtonian heating and internal heat generation/absorption. *PLoS One.* 2015;10(9):1–13. doi: [10.1371/journal.pone.0129613](https://doi.org/10.1371/journal.pone.0129613)